Proceedings of the 21st ICSMGE, Vienna, Austria, 14 – 19 June 2026. Pistrol, Adam & Schweiger (eds.)
Published by: ÖGG, Austrian Society for Geomechanics, Salzburg, Austria, ISBN 978-3-9503898-4-5
https://doi.org/10.53243/ICSMGE2026-336

Geotechnical characterization of a slope subsoil for seismic risk assessment purposes: the Chieuti case study.

Annamaria di Lernia,
Department of Engineering (DiIng), University of Basilicata, Italy; formerly, Department of Civil, Environmental, Land, Building Engineering and Chemistry (DICATECh), Technical University of Bari, Italy; annamaria.dilernia@unibas.it

Gaetano Elia
Department of Civil, Environmental, Land, Building Engineering and Chemistry (DICATECh), Technical University of Bari, Italy, gaetano.elia@poliba.it

ABSTRACT: One of the key points in the seismic risk assessment is the accurate prediction of the seismic shaking at ground surface, which is strongly affected by local site conditions including the uneven topography, the subsoil stratigraphy and the buried morphologies. The analysis of the local seismic response, usually performed through numerical simulations, is strongly dependent on the assumed geotechnical subsoil model, defined through site investigations and laboratory tests. The paper presents the geotechnical seismic characterization of the subsoil deposit of a landslide-prone natural slope, located in Chieuti, a little town in the north of Apulia (Southern Italy). The western slope of Chieuti is currently location of a deep, slow-moving paleo-landslide interacting with the urban area. The occurrence of a low-intensity earthquake in August 2018 induced an aggravation of the already diffuse landslide-related damage to the buildings and infrastructure at the crest of the slope. This prompted the execution of a detailed geotechnical and geophysical campaign, including boreholes, down-hole, seismic surface waves and resonant column tests to characterize the dynamic behaviour of slope soil for seismic risk assessment purposes. The paper discusses the integration and interpretation of the site and laboratory investigation data for the definition of the geotechnical subsoil model to be implemented in the numerical simulations of the local seismic response of the slope.

KEYWORDS: geotechnical characterization; cyclic/dynamic laboratory tests; in-situ investigations; seismic risk assessment; local seismic response.

1 GENERAL BACKGROUND OF THE SITE

The prediction of the seismic site response for the seismic risk assessment of a site is typically carried out through numerical models of different degrees of complexity, built to account for local site conditions. The accuracy of the predicted seismic response is strictly related to the reliability of the geotechnical subsoil model, which should contemplate the local stratigraphic conditions, the soil dynamic behaviour and the location of the seismic bedrock.

In this paper the geotechnical characterization of the seismic behaviour of the subsoil deposit of a landslide-prone natural slope has been conducted for seismic risk assessment purposes. The site of reference is the western slope of Chieuti (Foggia), a little town located in the south of Italy (Apulia Region – Figure 1a). The urban center is currently affected by a long-lasting instability phenomenon, damaging structures and infrastructures since the first decades of 1800 (Pagano et al., 2023; Sonnessa et al., 2023; Santaloia et al., in prep.). Indeed, the western side of the slope is location of a deep, slow-moving ancient landslide, whose current activity is mainly related to static actions. The phenomenological interpretation of the landslide mechanism, based on field and laboratory measurements of slope factors, geomorphological data, PS-InSAR data, analysis of structural damages and inclinometer results, revealed that the landslide is the result of a failure process initiated in the geological past, characterized by a retrogressive and deep-seated slip surface (Tagarelli et al., 2025; Santaloia et al., in prep.).

After an earthquake of low intensity occurred on the 16th of August 2018, the landslide-related damage affecting buildings and roads have been observed to be aggravated. This prompted an in-depth understanding of the seismic wave propagation processes affecting the slope during earthquakes, since the area is characterized by complex geological, topographic and stratigraphic conditions. Moreover, the site is located in a medium-to-high seismicity area, due to the proximity to different strike-slip faults, such as the Apricena and Mattinata faults (Patacca and Scandone, 2004). Indeed, according to the Italian seismic hazard map, the Chieuti area is characterized by a PGA between 0.175g and 0.225g on the outcropping rock for a return period of 475 years. Thus, the impact of earthquake events on the slope might be considered significant, requiring further in-depth investigation.

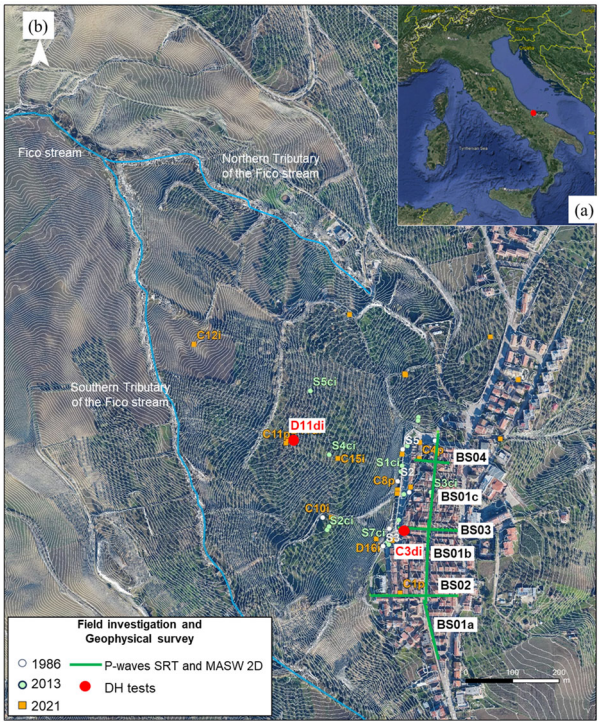

Figure 1. (a) The town of Chieuti in the Italian territory and (b) the western slope of Chieuti with the location of the field surveys conducted between 1986 and 2021.

2 IN-SITU AND LABORATORY INVESTIGATIONS

The characterization of the Chieuti western slope was carried out through several geotechnical in-situ surveys conducted since 1986 (Figure 1b). The most recent investigation campaign was conducted between November 2020 and March 2021, based on which the interpretation of the landslide mechanism and the diagnosis of the slope factors was conducted. The 2020-2021 geognostic campaign consisted in the execution of 21 vertical boreholes, equipped with both inclinometers and piezometers; execution of geophysical in-situ testing, i.e. two down-hole (DH) tests, P-waves seismic refraction (SRT) and 2D Multi-channel Analyses of Surface Waves (MASW 2D) tests along four alignments, for the reconstruction of the subsoil model and the characterization of the dynamic behaviour of the slope soils; retrieval of several soil samples for the mechanical and dynamic characterization. The location of the boreholes and the geophysical tests, executed during the recent site investigation, is depicted in Figure 1b, together with those carried out during the previous geognostic campaigns performed in 1986 and 2013 within the same area.

The DH tests were executed along the C3di (48 m deep) and D11di (70 m deep) boreholes, located within the town and in the middle of the western slope, respectively (Figure 1b). The seismic surface wave tests were conducted along one longitudinal (BS01) and three transversal (BS02, BS03 and BS04) alignments, crossing the urban center (Figure 1b). Since the longitudinal BS01 alignment was very long, it was divided into three consecutive alignments, named BS01c, BS01b and BS01a from south to north. The MASW2D tests used multiple equally-spaced receivers, placed along linear alignments and acquiring signals from an active impulsive source, in order to obtain 7 or 15 shear wave velocity V_S profiles along each section.

In addition to physical and mechanical tests conducted on 54 undisturbed soil samples to identify the index properties, compressibility and shear strength parameters, resonant columns (RC) tests were executed on 10 undisturbed soil samples to investigate the nonlinear cyclic response of the slope soils. The RC tests consisted of a first stage of isotropic consolidation, followed by a free-fixed dynamic excitation. The consolidation stage was carried out at the in-situ mean effective confining pressure p′, evaluated for each soil sample assuming a coefficient of earth pressure at rest K_0 equal to 1, unit weight constant with depth and equal to 19 kN/m^3 and the water level detected during the perforation of the boreholes. Several shear cycles of increasing amplitude were applied to the specimens to cover the range of cyclic shear strain amplitude between 10^{-4}% and $2 \cdot 10^{-1}$%, also measuring the excess porewater pressures during the tests.

3 GEO-LITHOLOGICAL SETTING OF THE SLOPE

The comprehensive analysis and integration of all the acquired data allowed to reconstruct the geological and lithological setting of the western slope of Chieuti (Santaloia et al., in prep.). The geological setting is characterized, from the bottom to the top, by the Montesecco Clays (Upper Pliocene-Lower Pleistocene), the Serracapriola Sands (Lower Pleistocene) and the Campomarino Conglomerates (Middle Pleistocene). The Montesecco Clays formation consists of marine blue-grey clays with thin intercalations of silty sand; the Serracapriola Sands are composed of sand and silt; the Campomarino Conglomerates consists of gravels dispersed within a clayey-silty matrix, deposited in an alluvial environment. The old urban center is built above the top-hill thinner continental layer belonging to the Campomarino Conglomerates, outcropping upslope and underlain by the marine succession of the Serracapriola Sands and the Montesecco Clays formations (Bracone et al., 2012).

The integration of the soil corings data and the geotechnical properties of the soil samples allowed the identification of three main soil units within the slope, spatially distributed as illustrated in the geo-lithological map reported in Figure 2 (Santaloia et al., in prep.). Specifically, Unit 1, belonging to the Campomarino Conglomerates formation, outcrops within the urbanized area; Unit 2, corresponding to the Serracapriola Sands, is subdivided into two Sub-units, i.e. an upper sandy unit, including local intercalation of gravel bodies (Sub-unit 2a) and a lower silty-sandy unit (Sub-unit 2b); Unit 3, associated to the Montesecco Clays formation, consists of blue-grey silty-clayey successions with rare sand intercalations. Within the western slope, the Unit 1 thickness ranges from 5 to 7 m, while the thicknesses of the Sub-unit 2a and 2b layers vary between 8–10 m and 15–20 m, respectively. The transition from Sub-unit 2b to the underlying Unit 3 tends to gradually deepen from south to north.

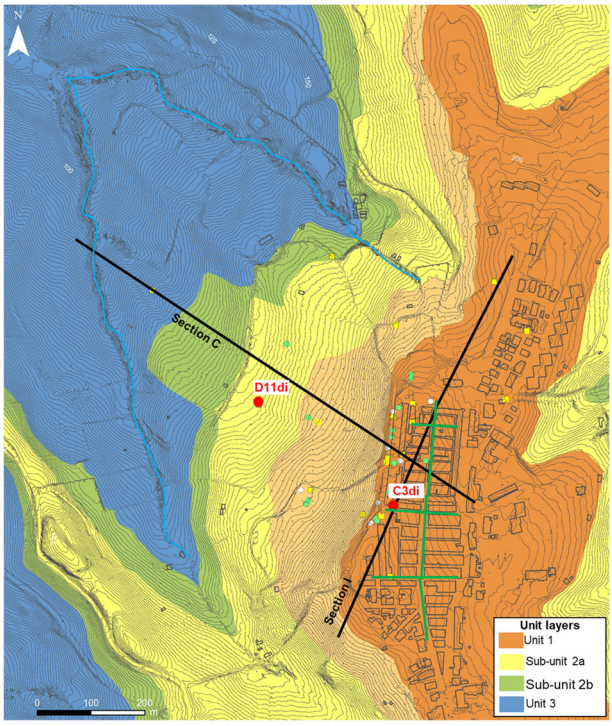

Figure 2. Geo-lithological map of the western slope of Chieuti with the location of the longitudinal and transversal sections (modified after Santaloia et al., in prep.).

4 RECONSTRUCTION OF THE GEOTECHNICAL SUBSOIL MODEL

The joint interpretation of P-waves SRT, DH and surface wave seismic tests allowed the identification of the subsurface model and the dynamic characterization of the soil unit layers, overcoming some of the limitations of the different seismic methods. Indeed, surface wave methods allow the identification of hidden layers, gradual velocity variations, velocity inversions and the effect of a shallow water table, which cannot be detected by refraction techniques. On the other hand, the P-waves refraction tests provide information on the bedrock position, lateral variation of velocities and water table depth. The geotechnical characterization of the slope soils is, then, completed by the investigation of their nonlinear dynamic response, carried out through resonant column (RC) tests on samples taken along different boreholes at various depths.

4.1 *Definition of S-wave velocity profiles*

The results of the DH tests for each borehole are reported in Figure 3, together with the corresponding stratigraphic logs obtained from the analysis of the continuous coring boreholes C3di and C11p very close to D11di. The MASW2D results (grey lines), referring to different verticals along each alignment and representing the response of the soil deposit below the entire urban area, are also shown in Figure 3a. For both verticals, a gradual variation with depth of the P- and S-waves velocity can be observed, with a clear demarcation at the stratigraphic contacts between different soil layers.

More specifically, the DH test conducted within the urban area (Figure 3a) allowed to identify the presence of a first 1 m thick soil layer with a V_S of about 200 m/s, representing the man-made soil, followed by a layer of about 300 m/s ascribable to Unit 1 down to the depth of 5-7 m below ground level (b.g.l.). Then, V_S gradually increases up to 30 m b.g.l., where the Sub-unit 2a and 2b layers are encountered; the transition between the Sub-unit 2a and 2b is not significantly pronounced, probably due to the strong heterogeneity of the soil deposit in the upper portion of the slope, already recognized by other stratigraphic logs in the same area (Santaloia et al., in prep). Where the Montesecco clays are encountered, the S-wave velocity profile increases to values ranging between 700 and 1200 m/s, the latter reached at the depth of 42 m. A similar trend is observed for different verticals within the urban area as retrieved from MASW2D tests.

In the mid portion of the slope, the D11di wave velocity profiles (Figure 3c) show an overall increasing trend with depth and a clear demarcation at the stratigraphic contacts between different soil layers. The first layer down to 7 m b.g.l is associated with the Sub-unit 2a, as also suggested by the stratigraphic log of the close C11p borehole. Then, a layer characterized by 600 m/s is ascribed to the Sub-unit 2b down to 18 m b.g.l. Below this depth, the Unit 3 layer is characterized by increasing V_S values ranging from 800 m/s to about 1200 m/s, the latter detected at a depth of 52 m b.g.l. A velocity inversion is observed within the Sub-unit 2b at depths between 12.2 m and 16.8 m.

Normalizing the corresponding shear stiffness modulus G_0 profiles by the confining pressure p′ (Figure 3b, d), it might be observed that soils in the D11di borehole are overall stiffer than those present along the C3di vertical. With reference to the D11di stratigraphic profile, the sandy member of the Sub-unit 2b (between 7 and 12.2 m depth) is characterized by a G_0/p' ratio significantly higher than the value evaluated along the C3di profile in the same layer (between 18 m and 25 m). Moreover, the G_0/p' ratio for the silty member of Sub-unit 2b along C3di (between 25 and 30 m depth) results to be higher than that obtained for the same soil layer in D11di (between 12.2 and 16.8 m depth). This indicates that, on one side, the sandy member of Sub-unit 2b in the borehole D11di is significantly stiffer with respect to the underlaying silt member; on the other side, the silty member in D11di is particularly less stiff than the same material along the C3di profile. This circumstance might be justified by the concurrence of two effects, i.e. the strong lithological heterogeneity discovered between 7 and 12.2 m during the stratigraphic analysis and the possible presence of a shear band at a depth between 12.2 and 16.8 m, which contributes to reduce the stiffness of the material (di Lernia et al., 2023).

The seismic geophysical tests clearly suggested that Unit 3 might be subdivided into to two sub-layers according to their dynamic response: a first one characterized by an average value of the shear wave velocity of about 800 m/s found at depth lower than 50 m b.g.l., and a very stiff layer of Unit 3 having an average V_S of about 1200 m/s for depths higher than 50 m b.g.l.

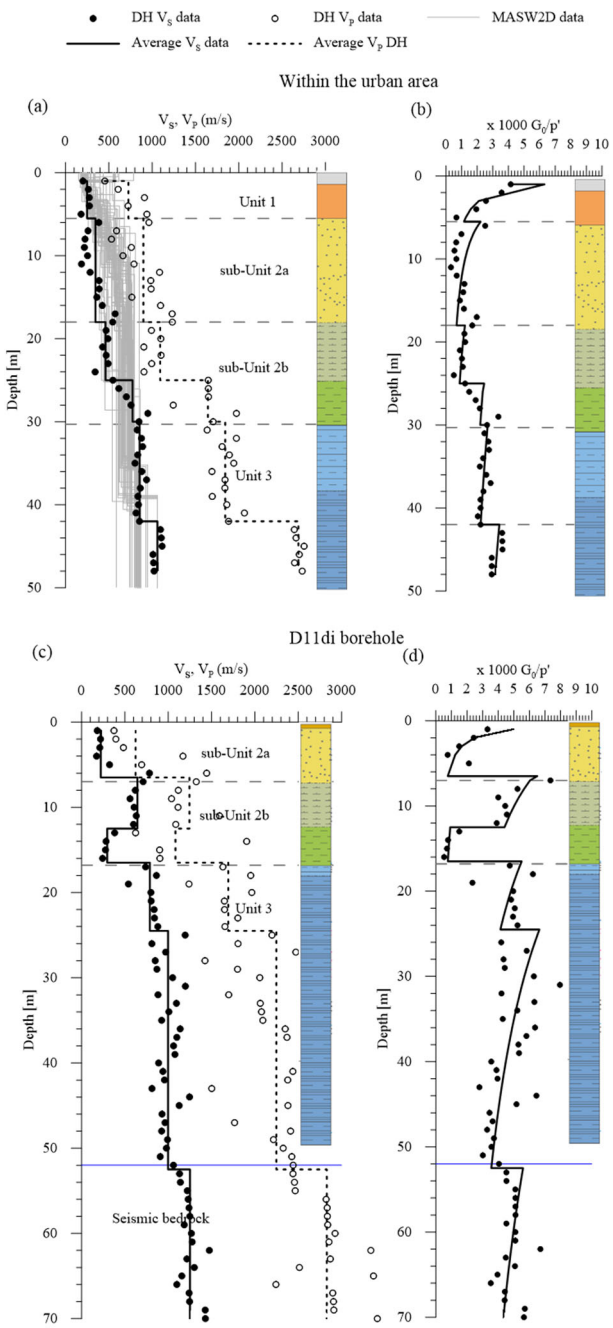

Figure 3. S- and P- wave velocity profiles and normalized shear stiffness modulus G_0/p' along the (a, b) C3di and (c, d) D11di boreholes as retrieved by down-hole tests. In subplot (a), the V_S profiles obtained through MASW2D tests are also shown.

The different behavior for the shallower and deeper portions of Unit 3 is also highlighted by RC results, as shown in terms of shear modulus and damping ratio decay curves later on. This evidence guided the identification of the location of the seismic bedrock, defined as the stratigraphic contact at which the shear wave velocity V_S is greater than 1200 m/s.

Based on these in-situ investigations results, the dynamic geotechnical model of the western slope of Chieuti was defined by assigning a constant value of the S-wave velocity to each lithological unit, determined as an average value of the available measured data, as summarized in Table 1.

Table 1. Shear wave velocity for each soil unit.

Soil unit	Man-made soil	Unit 1	Sub-unit 2a	Sub-unit 2b	Unit 3	Very stiff Unit 3
V_S (m/s)	200	317	491	627	871	1250

4.2 *Interpretation of P-waves seismic refraction tests*

The analysis of P-waves seismic refraction tests, along with the stratigraphic boreholes and down-hole tests, allowed the reconstruction of the litho-stratigraphic succession and the morphology of the stratigraphic contacts for those areas not directly crossed by boreholes. The P-waves SRT tomography retrieved along the longitudinal BS01 alignment only is reported in Figure 4, for brevity. The cross correlation of data obtained by longitudinal and transversal sections allowed to identify the stratigraphic contacts between different layers: the stratigraphic contact between Sub-unit 2a and 2b layers is found at about 25 m in the southern sector and tend to deepen at about 30 m in the northern area. A stiffer portion might be observed in the middle sector of the section, ascribable either to the presence of the same material in a different densification state or to the presence of a different material. It should be mentioned that this area of the slope is mostly affected by the retrogressive nature of the landslide mechanism.

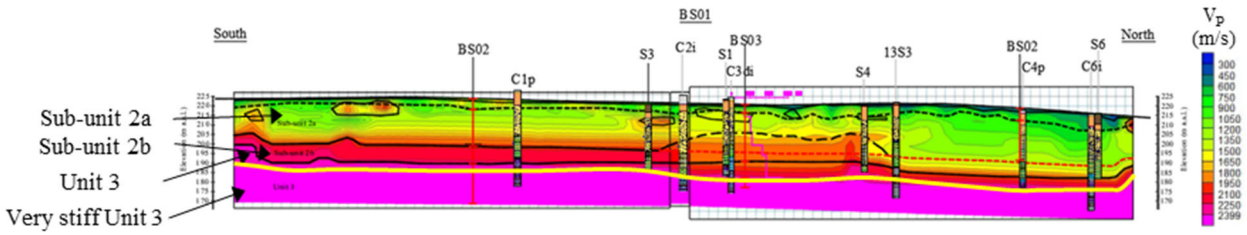

Figure 4. 2D profile of the P-wave seismic refraction tests BS01 along the urban center.

Going from south to north, also the stratigraphic contact between Unit 2 and Unit 3 tends to deepen from about 30 m b.g.l. in the southern area to about 35 m in the northern area. The top of the stiffer portion of Unit 3 (yellow line in Figure 4), representing the seismic bedrock, was identified at about 50 m b.g.l. along the longitudinal section, based on both C3di DH data and the P-wave seismic tomography retrieved along the transversal sections. It derives that the Unit 3 layer has a variable thickness going from south to north, reaching maximum values in the middle portion of the longitudinal section between boreholes C2i and 13S3ci.

Overall, the geophysical investigation recognized a significant weakening of soils within the northern sector of the slope, where the landslide mechanism is mostly affecting the area. Indeed, seismic tomography gave evidence to a lowering of the portion characterized by low stiffness moving from south to north.

4.3 *Soil cyclic response from RC tests*

The cyclic nonlinear response of the slope soils was investigated through the resonant column tests performed on 10 undisturbed samples retrieved from 8 different boreholes. Specifically, a total of 10 samples were tested, among which one (i.e. C6iA2) belonging to Unit 1, three (i.e. C5i/CI2b, C9i/B2 and C10i/A2) belonging to Sub-unit 2b and six (i.e. C3di/E2, C10i/B2, C13i/D2, C7p/B2, C15i/A2 and C15i/B2) belonging to Unit 3, as summarized in Table 2. Only for the sample C6i/A2, two specimens were prepared, one consolidated to the in-situ mean effective confining pressure and the other confined to twice this value. It should be mentioned that the preparation of undisturbed specimens of Sub-unit 2a unit was not possible due to the non-cohesive nature of the soil; thus, no decay curves are available for this unit.

According to the particle size distribution (Figure 5), Unit 3 and Sub-unit 2b samples can be classified as sandy silts and silty sands with a low percentage of clay fraction (between 15% and 29%). The only sample whose curve is outside the Unit 3 granulometric envelope is the C15/B2, characterized by a higher percentage of clay fraction, which was retrieved within the very stiff portion of Unit 3. Also, the C6i/A2 sample of Unit 1 is characterized by a high percentage of coarse-grained soil with many inclusions of fine particles. Most of the specimens are characterized by a plasticity index (PI) ranging from 10% to 20%, except for C15/B2 and C6i/A2 having PI equal to 30% and 40%, respectively.

Table 2. Characteristics of the 10 samples tested in the resonant column.

Sample	Unit	Depth (m)	γ_{sat} (kN/m^3)	e_0 (-)	w (%)	PI (%)	CF (%)
C6i/A2	1	5.5-6	19.495	0.683	23.4	39.8	28.8
C10i/A2	2b	16.5-17	19.51	0.639	20.7	12.9	16
C5i/CI2b	2b	17.4-17.5	18.9	0.772	26.4	10.7	16
C9i/B2	2b	24.0-24.5	19.15	0.725	24.7	17.3	28
C10i/B2	3	23-23.5	20.13	0.601	21.7	14.9	17.4
C15i/A2	3	31.5-32	19.97	0.605	21	11.8	14.6
C7p/B2	3	32.5-33	19.7	0.647	22.5	16.6	16.55
C3di/E2	3	35.5-36	19.38	0.684	23.2	17.7	19.5
C15i/B2	3	45.5-46	19.71	0.669	24.2	30	42.5
C13i/D2	3	50.50-51	19.51	0.639	20.7	19.6	21.6
C6i/A2	1	5.5-6	19.495	0.683	23.4	39.8	28.8
C10i/A2	2b	16.5-17	19.51	0.639	20.7	12.9	16

The RC experimental results are plotted in Figure 6 in terms of normalized shear modulus, G/G_0, damping ratio, D, and excess porewater pressure, Δu, variation with the shear strain, γ (%). The decay curves suggested by Vucetic and Dobry (1991) for soils with PI equal to 0% and 50%, representing a lower and upper limit for the present case study, are reported for comparison in the same figure. As typically observed, soils with high PI values are characterized by higher G/G_0 at a given γ and, as a consequence, a higher linear shear strain threshold (Darendeli, 2001). With reference to the damping curves D-γ, at small strains soils with high PI exhibit high initial values, while the damping ratio values tend to cross over the curves relative to soils with low PI for increasing shear strain levels. Conversely, soils with low PI tend to exhibit low damping ratios at very small strains and higher D values within the small to medium strain range (Ciancimino et al., 2020; Lanzo and Vucetic, 1999).

The excess porewater pressure chart (Figure 6c) clearly shows the expected tendency of low plasticity soils to develop high values of Δu for lower shear strain levels. Indeed, soils

with low PI are characterized by a low volumetric shear strain threshold; as PI increases, the cyclic shear strain amplitude below which no permanent cyclic porewater pressure is recorded tends to increase (Mortezaie and Vucetic, 2016).

For the Unit 1 samples, the dependence of the soil nonlinear behavior on the clay fraction and plasticity index is evident. The high PI (equal to 40%) due to the relevant CF (equal to 28.8%) contributes to enlarging the linear strain threshold, which increases for increasing confining pressures. Indeed, the linear strain threshold is about 10^{-3}% for the C6i/A2a specimen consolidated to 100 kPa and it increases to $3 \cdot 10^{-3}$% for a confining pressure of 200 kPa. This tendency also reflects on the volumetric strain threshold, characterized by values in the order of $5 \cdot 10^{-2}$%. The initial damping ratio D_0 is about 5%, due to the high PI and to the significant percentage of clay fraction. The trend of the shear stiffness modulus decay curves is within the envelope proposed in the literature for a PI between 30% and 50%.

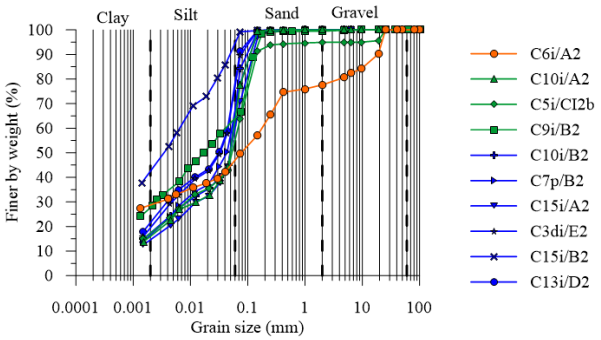

Figure 5. Particle size distribution of the tested soil samples.

With reference to Sub-unit 2b, a similar trend in terms of normalized shear stiffness modulus curves can be recognized for C5i/CI2b and C9i/B2 samples, for which the linear strain threshold is about $2 \cdot 10^{-3}$%, while the volumetric strain threshold is about $3 \cdot 10^{-2}$%. The initial damping ratio D_0 is about 3%, consistently with their low plasticity index. A different behaviour is observed for the C10i/A2 sample, characterized by a greater reduction of the shear stiffness at the same shear strain level with respect to the other samples and a lower volumetric threshold value (equal to 10^{-2}%). This behaviour could not be attributed solely to the plasticity index, as the PI values are almost similar for all the Sub-unit 2b samples. The different nonlinear response shown by the C10i/A2 sample could be rather related to its soil composition, as the sample was retrieved within the transition zone between the Sub-unit 2b and Unit 3. Indeed, the grain size distribution curve of C10i/A2 is similar to that of C10i/B2, retrieved at a higher depth along the same borehole within Unit 3. In fact, the nonlinear behaviour of the C10i/A2 specimen resembles that obtained for the C10i/B2 sample, in terms of shear stiffness modulus, damping ratio curves and excess porewater pressure varying with the shear strain. This circumstance suggests that the C10i/A2 sample might be associated, for its cyclic response, to Unit 3.

The analysis of the RC results for Unit 3 soils highlights a great dispersion in their nonlinear behaviour, exhibiting linear thresholds increasing with the plasticity index. Most of the normalized shear stiffness modulus decay curves lie within the enveloped proposed in the literature for a PI between 15% and 30%. Differently from the other specimens, the response of the sample C15i/B2 shows a wider pseudo-linear strain range, strictly related to its higher plasticity index (equal to 30%) and clay fraction (equal to 42.5%). As a consequence, the volumetric threshold attains a value of about $4 \cdot 10^{-2}$%, which is higher than that pertaining to the other Unit 3 samples, i.e., 10-2%. In all cases, the initial damping ratio D_0 is about 2-3%.

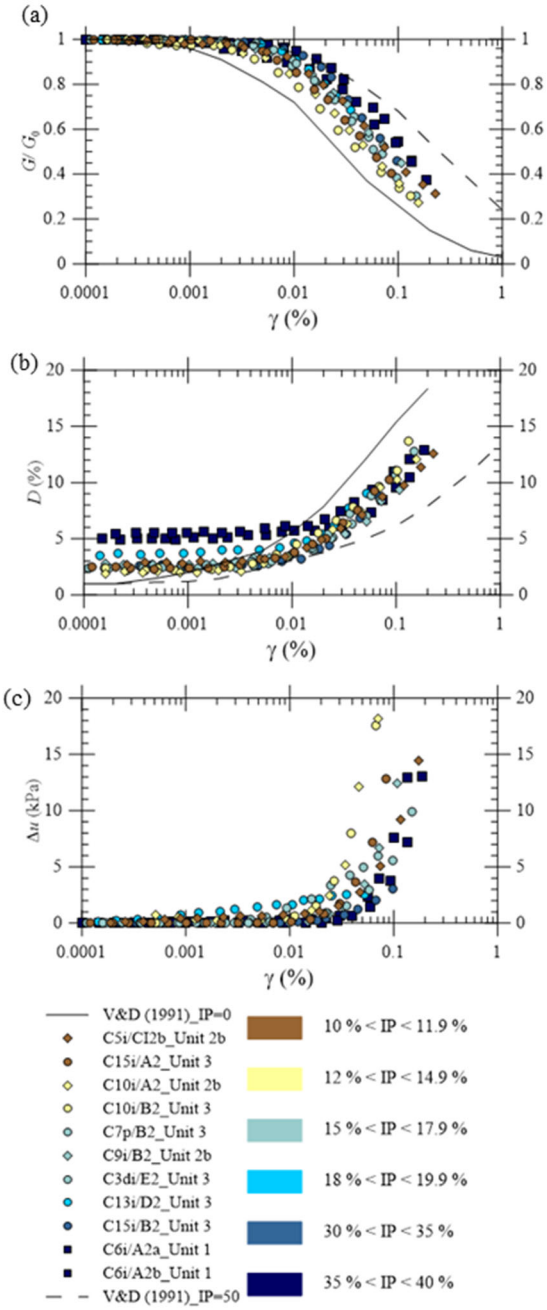

Figure 6. Results of all the RC tests in terms of normalized shear modulus, damping ratio and excess porewater pressure curves plotted as a function of PI and compared to the Vucetic and Dobry (1991) (V&D (1991)) curves for PI equal to 0% and 50%.

The RC experimental data were compared to the results obtained from the in-situ geophysical investigations, i.e., DH and MASW2D tests. In particular, the shear wave velocity determined through RC tests, $V_{s,lab}$, was compared to the in-situ S-wave velocity, $V_{s,field}$, measured at the corresponding depth along verticals close to the boreholes from which the RC samples were retrieved. The laboratory shear wave velocity $V_{s,lab}$ was determined from the value of the initial shear stiffness modulus G0 measured at the smallest strain levels reached during the RC tests on the samples C6i/A2a, C9i/B2 and C3di/E2. The comparison, shown in Figure 7, indicates that the laboratory data are considerably lower than the field

ones, since the ratio $V_{s,lab}/V_{s,field}$ is equal to 0.35 for the C3di/E2 sample, 0.38 for C6i/A2 and 0.45 for C9i/B2.

This discrepancy might be ascribed to soil disturbance due to the sampling procedures and to other experimental factors, such as the re-consolidation technique and the loading frequencies. Indeed, it is widely recognized that shear wave velocity measured in the laboratory might be considerably lower than the corresponding in-situ value. This loss in stiffness can be related to the irrecoverable damages at the interparticle contacts caused by sampling, resulting in an alteration of the soil structure (Ciancimino et al., 2020; d'Onofrio et al., 2009; Foti et al., 2001; Stokoe and Santamarina, 2000). As already observed in the literature, the ratio $V_{s,lab}/V_{s,field}$ reduces as the field shear wave velocity increases, implying that the sample disturbance effects are, on average, more relevant for soils characterized by higher $V_{s,field}$.

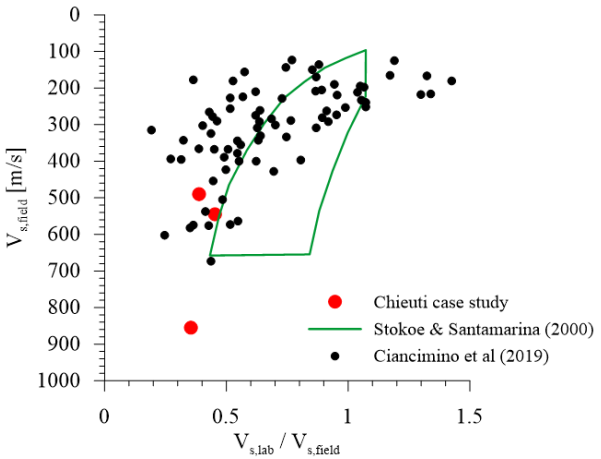

Figure 7. Variation of $V_{s,lab}/V_{s,field}$ with $V_{s,field}$ as obtained from experimental data presented in the literature (modified from Ciancimino et al. (2020) and Stokoe and Santamarina (2000)) and for the Chieuti case study.

5 CONCLUDING REMARKS

The paper presents the seismic geotechnical characterization of a landslide-prone slope for the seismic risk assessment of the area. The site of reference is the western slope of Chieuti (Foggia, Apulia Region), characterized by complex geological and topographic conditions for which important seismic amplification effects are expected. For this reason, it is important to accurately define the geotechnical seismic model to be implemented in the numerical analyses for the prediction of the seismic slope response. To this purpose, in-situ geophysical surveys (i.e. seismic surface and down-hole tests) and laboratory tests (i.e. resonant column tests) were carried out. The joint interpretation of the site investigations allowed to define the subsoil geotechnical model, in terms of morphology of stratigraphic contacts, location of the seismic bedrock and dynamic properties of the slope soils. The so-defined geotechnical model will serve as the basis for the construction of the numerical model and the calibration of the soil constitutive models to be used in the seismic response analysis of the slope area. The final aim will be to produce maps of amplification factors at ground surface, identifying those areas characterized by the highest hazard due to local site conditions (di Lernia et al, in prep.).

6 ACKNOWLEDGEMENTS

The project "S.I.S.M.A.: Seismically Induced Slope Movements Acceleration", funded by the Italian Ministry of University and Research in the context of the PRIN 2022 PNRR (CUP_D53D23018050001) is kindly acknowledged. G. Elia is grateful for the financial support provided by the European Union – Next Generation EU within the National Recovery and Resilience Plan, Mission 4_2_1.4. in the framework of the "National Centre for HPC, Big Data and Quantum Computing – Spoke 5: Environment and Natural Disasters" (CN_00000013).

7 REFERENCES

Bracone, V., Amorosi, A., Aucelli, P.P.C., Rosskopf, C.M., Scarciglia, F., Di Donato, V., Esposito, P. 2012. The Pleistocene tectono--sedimentary evolution of the Apenninic foreland basin between Trigno and Fortore rivers (Southern Italy) through a sequence-stratigraphic perspective. *Basin Research* 24, 213–233.

Ciancimino, A., Lanzo, G., Alleanza, G.A., Amoroso, S., Bardotti, R., Biondi, G., Cascone, E., Castelli, F., Di Giulio, A., d'Onofrio, A., Foti, S., Lentini, V., Madiai, C., Vessia, G. 2020. Dynamic characterization of fine-grained soils in Central Italy by laboratory testing. *Bulletin of Earthquake Engineering* 18, 5503–5531.

d'Onofrio, A., Vitone, C., Cotecchia, F., Puglia, R., Santucci de Magistris, F., Silvestri, F. 2009. Caratterizzazione geotecnica del sottosuolo di San Giuliano di Puglia. *Italian Geotechnical Journal* 3, 43–61.

Darendeli, M.B. 2001. *Development of a New Family of Normalized Modulus Reduction and Material Damping Curves*. PhD Thesis, University of Texas, Austin.

di Lernia, A., Buono, C., Elia, G. 2023. Evaluation of seismic site effects in a real slope through 2D FE numerical analyses. *Proc. 9th International Conference on Computational Methods in Structural Dynamics and Earthquake Engineering - COMPDYN 2023*. pp. 4110–4124.

di Lernia, A., Papadimitriou, A.G., Reina, A., Elia, G. Nonlinear FE study of the seismic response of an urbanised slope with complex geo-lithological and topographic conditions for seismic hazard assessment purposes. *Soil Dynamic and Earthquake Engineering* (in prep.)

Foti, S., Lo Presti, D., Pallara, O., Rainone, M.L., Signanini, P. 2001. Indagini geotecniche e geofisiche per la caratterizzazione del sito di Castelnuovo Garfagnana (Lucca). *Italian Geotechnical Journal* 3, 42–60.

Lanzo, G., Vucetic, M. 1999. Effect of Soil Plasticity on Damping Ratio at Small Cyclic Strains. *Soils and Foundation* 39, 131–141.

Mortezaie, A., Vucetic, M. 2016. Threshold Shear Strains for Cyclic Degradation and Cyclic Pore Water Pressure Generation in Two Clays. *Journal of Geotechnical and Geoenvironmental Engineering* 142, 04016007.

Pagano, N., Sonnessa, A., Cotecchia, F., Tarantino, E. 2023. Integrated Use of Geomatic Methodologies for Monitoring an Instability Phenomenon. *Lecture Notes in Computer Science (Including Subseries Lecture Notes in Artificial Intelligence and Lecture Notes in Bioinformatics)* 14107, 217–233.

Patacca, E., Scandone, P. 2004. The 1627 Gargano earthquake (Southern Italy): Identification and characterization of the causative fault. *Journal of Seismology* 8, 259–273.

Santaloia, F., di Lernia, A., Tagarelli, V., Sonnessa, A., Guglielmi, S., Bottiglieri, O., Pisano, L., Stragapede, M., Tarantino, E., Elia, G., Cotecchia, F. Challenges in the diagnosis of a very slow paleo-landslide for mitigation purposes. *Engineering Geology* (in prep.)

Sonnessa, A., di Lernia, A., Oscar Nitti, D., Nutricato, R., Tarantino, E., Cotecchia, F. 2023. Integration of multi-sensor MTInSAR and ground-based geomatic data for the analysis of non-linear displacements affecting the urban area of Chieuti, Italy. International *Journal of Applied Earth Observation and Geoinformation* 117, 103194.

Stokoe, K.H., Santamarina, J.C. 2000. Seismic-Wave-Based Testing In Geotechnical Engineering. *International Society for Rock Mechanics (Ed.), ISRM International Symposium*.

Tagarelli, V., Santaloia, F., Elia, G., Cotecchia, F. 2025. Numerical modelling of geological processes as means for the diagnosis of ancient landslide mechanisms. *Computers and Geotechnics* 107238

Vucetic, M., Dobry, R. 1991. Effect of Soil Plasticity on Cyclic Response. *Journal of Geotechnical Engineering* 117 (1), 89–107.